Journal of Biomedical Optics

SPIEDigitalLibrary.org/jbo

Study of dynamic pressure-induced refractive index change using derivative total reflection method

Jin Wang
Qing Ye
Zhichao Deng
Tengqian Sun
Wenyuan Zhou
Jianchun Mei
Chunping Zhang
Jianguo Tian

SPIE

Study of dynamic pressure-induced refractive index change using derivative total reflection method

Jin Wang, Qing Ye, Zhichao Deng, Tengqian Sun, Wenyuan Zhou, Jianchun Mei, Chunping Zhang, and Jianguo Tian
Nankai University, School of Physics and TEDA Applied Physics School, MOE, Key Laboratory of Weak-Light Nonlinear Photonics, Tianjin 300071, China

Abstract. We report the dynamic refractive index (RI) change of tissue under a stepped compression load using a custom-built pressure apparatus. Angle-dependent reflectance profiles of biotissue samples are recorded, and the RI values are resolved using the derivative total reflection method. These results are relevant for understanding the mechanism of mechanical optical clearing, for investigating tissue dynamics under mechanical stimuli, and for other biomedical applications. [DOI: 10.1117/1.JBO.18.11.117005]

Keywords: refractive index; total reflection; optical clearing; pressure.

Paper 130409R received Jun. 13, 2013; revised manuscript received Aug. 31, 2013; accepted for publication Oct. 1, 2013; published online Nov. 8, 2013.

1 Introduction

The concept of reducing the optical scattering in tissue to enhance the effectiveness of diagnostic and therapeutic treatments has stimulated research in the optical clearing (OC) technique since 1997.[1,2] Previous studies have mainly focused on the use of biocompatible and osmotically active chemical agents.[3,4] As an important candidate mechanism of OC technique, some researchers shed light on another alternative nonchemical technique of mechanical compression in recent years, which creates fast local effects, maintains stratum corneum integrity and may be harnessed as a minimally invasive OC technique.[5–8] In the previous work, laser beam profiles in response to mechanical compression were measured with experiments carried out on uniform compression between two glass slides, so the compressive force applied to the tissue was unknown.[5] Other techniques have been applied for evaluating the effect of OC under direct mechanical compression, such as image analysis,[6] optical coherence tomography,[7] and diffuse reflectance spectroscopy.[8] However, these previous studies have largely focused on transmission or reflection light intensity measurements. A direct and systematic evaluation of mechanical OC effect has not yet been achieved. As the most direct parameter for OC effect evaluation, the change in refractive index (RI) as a function of pressure is required.

On the other hand, for optical properties measurements of biotissue, an appropriate means for applying and maintaining pressure during experiments is required to keep surface tissues immobile, to achieve precise and reproducible treatment of the tissue, and to minimize any related noise contributions.[9] In one study involving several laboratories,[10–12] reflectance measurements and the inverse double method were used to find the relationship between the optical parameters (mainly the reduced scattering and absorption coefficients) and the pressure, whereas a direct study of RI was not attempted. The RI of tissue, as an indicator of the presence of tumors, has gained significant attention in recent years.[13] The study of tissue dynamics under mechanical stimuli has provided another impetus to use pressure-induced tumor structural and functional dynamic characteristics for the detection of cancer.[14] Knowledge of the change in the dynamic RI of biotissue over a wide pressure range is crucial for these reasons.

The pioneering work of Ding et al. first reported a change in RI with respect to skin sample pressure for applied pressures of <0.55 MPa.[15] In this article, we report measurements of the change in the dynamic RI of tissue under a stepped compression load (0 to 2.1 MPa) using a custom-built pressure apparatus. Angle-dependent reflectance intensity profiles were measured, and dynamic RI values of tissue were resolved under different pressures using the derivative total reflection method (DTRM). The relationship between the change in RI, the reduction of tissue fluid, and applied pressure is reported. These results are valuable for the evaluation of the mechanical OC effect and provide previously unreported RI values for tissue under applied pressure.

2 Materials and Methods

The experimental setup used in this work is shown in Fig. 1 and is based on our previously reported work.[16] The setup consists of a He-Ne laser (632.8 nm), rotation stage (M-038, Physik Instrumente, Germany), half-wave plate H, polarizer P, aperture diaphragm D, and dual-channel power meter (PM320E, Thorlabs, New Jersey, USA) with two detectors (PD1 and PD2). The effect of fluctuations in the laser power is minimized by the beam splitter M and by the continuous monitoring of the laser power by PD1. Our custom-built pressure apparatus consists of an air pump, a piston-cylinder, and an air gauge to monitor the pressure. An aluminum plate attached to a reciprocating piston can move forward and backward to generate stepped compression loads of 0.35, 0.70, 1.05, 1.4, 1.75, and 2.1 MPa. Samples filled in a plastic groove were sandwiched between the aluminum plate and an equilateral prism and then fixed on the rotation stage. With the aid of a Mercury

Address all correspondence to: Qing Ye and Jianguo Tian, Nankai University, School of Physics and TEDA Applied Physics School, MOE, Key Laboratory of Weak-Light Nonlinear Photonics, Tianjin 300071, China. Tel: 86-22-23503697; Fax: 86-22-23508379; E-mail: yeqing@nankai.edu.cn; jjtian@nankai.edu.cn

0091-3286/2013/$25.00

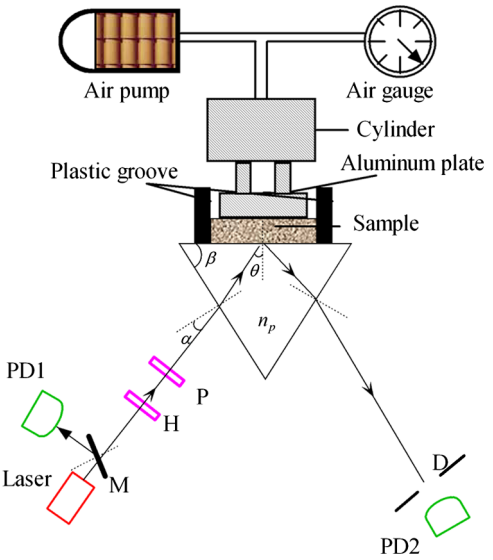

Fig. 1 Schematic diagram of the experimental setup.

C-863 servo motor controller and the PI General Command Set software on a computer, the prism was rotated with different incident angles. The reflectance intensity profile collected by PD2 was recorded as a function of incident angle. The illuminated area is inside a circle of radius about 3 mm. Porcine and bovine leg muscles were obtained from the local abattoir immediately after slaughter. Fresh porcine muscle tissue was first frozen for 30 min and then trimmed to a thin section of about 1.2 cm radius and 2 mm thickness to fill the plastic groove. Each sample was measured for ambient and increasing pressures. Bovine tissue was prepared in the same way. The reflectance profile at each pressure was measured three times, and the calculated variation was found to be <3% for all measurements.

Previously, we found that there is a random distribution of tissue fluid and muscle tissue at the prism-tissue interface, while the RI information of tissue fluid and the muscle tissue can be extracted by reflectance measurement, respectively.[16] Either the tissue fluid or the muscle tissue can be considered to be homogeneous and to yield an average RI value. The measured reflectance is a result of two types of contact areas. Taking into account the tissue fluid, the reflectance is expressed as

$$R_s^+ = b_f R_f + b_m R_m, \tag{1}$$

where R_f and R_m are the reflectance from tissue fluid and muscle tissue surface, respectively; b_f and b_m are fractions of the tissue fluid and the muscle tissue, respectively, at the illuminated areas, and $b_f + b_m = 1$.

According to the Fresnel formula,[17] for transverse electric (TE) wave, R_f is given by

$$R_f = (1 - R_{1,2})^2 \times R_{2,3}, \tag{2}$$

$$R_{1,2} = \left\{\frac{\cos\alpha - n_1\cos[a\,\sin(\sin\alpha/n_1)]}{\cos\alpha + n_1\cos[a\,\sin(\sin\alpha/n_1)]}\right\}^2, \tag{3}$$

$$R_{2,3} = \left\{\frac{n_1\cos\theta - n_f\cos[\arcsin(n_1\sin\theta/n_f)]}{n_1\cos\theta - n_f\cos[\arcsin(n_1\sin\theta/n_f)]}\right\}^2, \tag{4}$$

where $R_{1,2}$ and $R_{2,3}$ denote the reflectance at the air-prism and prism–sample interface, respectively. n_f is the RI of tissue fluid. R_m can be calculated in a similar way by replacing n_f with the RI of muscle tissue n_m in Eqs. (2)–(4). According to the schematic diagram in Fig. 1, n_f and n_m can be solved by $n_f = n_1\,\sin[\beta \pm a\,\sin(\sin\alpha_{c,f}/n_1)]$ and $n_m = n_1\,\sin[\beta \pm a\,\sin(\sin\alpha_{c,m}/n_1)]$, respectively. As described above, a binary distribution of tissue fluid and muscle should result in a double peak on the derivative curve. $\alpha_{c,f}$ and $\alpha_{c,m}$ are the critical incident angles when total internal reflection occurs at the prism-liquid and prism-tissue interface, respectively, which correspond to the angular positions of the first and second maxima of the derivative curve. Similar equations exist for transverse magnetic (TM) wave. The amplitude of the first and second peak on the reflectance curve indicates the proportion of tissue fluid and muscle tissue in the illuminated area, respectively.[16]

The model described by Eq. (1) was fitted to a reflectance profile where b_1 and b_2 are fitting parameters. A nonlinear least-squares fitting program based on the Nelder–Mead simplex algorithm was implemented by MATLAB software, which minimizes the sum $S(N) = \sum_{i=1}^{N}[R_{m,i} - R_{s,i}^+]^2$. $R_{m,i}$ is the i'th measured reflectance. $R_{s,i}^+$ is the i'th calculated reflectance obtained by Eq. (1). The reliability of the fit is given by E_s^2, defined as $E_s^2 = 1 - \sum_{i=1}^{N}(R_{m,i} - R_{s,i}^+)^2 / \sum_{i=1}^{N}(R_{m,i} - \bar{R})^2$, where $\bar{R}$ is the mean value of measured reflectance over N values of incident angle. E_s^2 ranges from 0 to 1, where a value near 1 represents a reliable fit.

3 Results and Discussion

Figure 2(a) shows the measured reflectance data and the model fit for porcine tissue at different pressures. When pressure was applied to the sample, the RI of tissue fluid could be calculated using the value for the critical angle $\alpha_{c,f}$, which is about 51.8 deg. The amplitude of the first peak on the reflectance curve indicates the proportion of tissue fluid in the illuminated area. The derivative of the reflectance curves is shown in Fig. 2(b). The amplitudes of the first peak gradually disappear as the pressure increases. On account of the pressure effect, the loss of tissue fluid at the prism–tissue interface results in a decrease in the amplitude of the first peak. A large increase of $\alpha_{c,m}$ was observed, and n_m significantly increased from 1.373 to 1.450. The RIs of muscle and tissue fluid as a function of the pressure are shown in Fig. 2(c). n_f ranges from 1.335 to 1.352 under compression. No noticeable change in n_f was observed with an increase in pressure, whereas a noticeable increase in n_m was observed when the pressure was higher than 0.35 MPa. The proportions of tissue fluid are calculated and shown in Fig. 2(d). The proportion of tissue fluid reduced from 57.9 to 16.9% when the applied pressure was increased from 0 to 2.1 MPa. The calculated n_r of 1.373 at 0 MPa is similar to the reported values of porcine tissue.[18]

The RIs of bovine muscle and tissue fluid as a function of the pressure are shown in Fig. 3(a). n_f ranged from 1.335 to 1.357 under compression, and n_m increased from 1.382 to 1.434. The measured result under the condition of zero pressure is in close agreement with values reported.[19] In Fig. 3(b), an obvious reduction in tissue fluid can be observed at pressures >0.35 MPa, which resembles the porcine tissue results. The

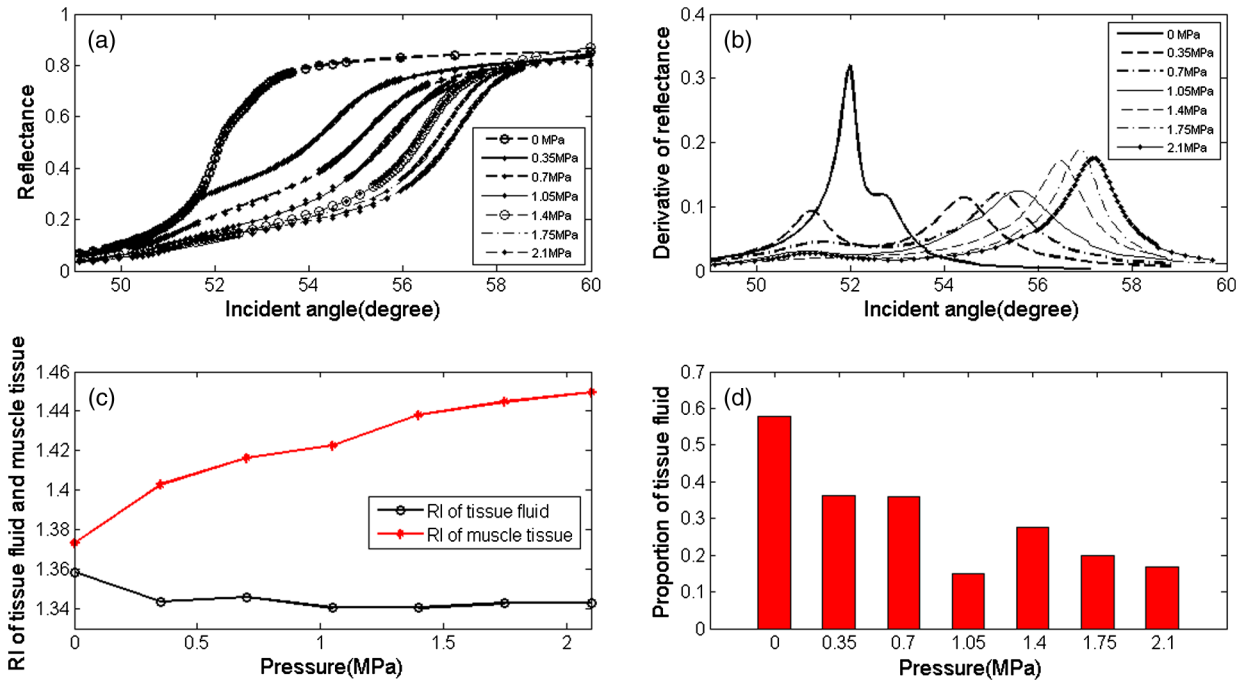

Fig. 2 (a) Measured reflectance data and fitting curves for porcine tissue under different pressure. (b) The derivative of the reflectance curves. (c) Refractive indices (RIs) of tissue fluid and muscle tissue versus the applied pressure. (d) Proportions of tissue fluid under different pressure.

proportion of tissue fluid b_f decreased from 79.5 to 25.9% for an increase in applied pressure from 0 to 0.35 MPa. When the pressure increased to 2.1 MPa, only about 6.9% of the total tissue fluid remained.

We define a relative displacement of tissue fluid Δm to record the loss of tissue fluid under different pressures. $\Delta m = [m(t) - m(0)]/m(0)$, $m(0)$ is the initial weight of tissue sample, $m(t)$ is the final weight of sample after a certain pressure was applied for 5 min. Here, 5 min is the average time in the reflectance measurement for each pressure. The result of Δm is shown in Fig. 4. We can find that the displacement of bovine tissue is much faster than the porcine tissue when the pressure first reached 0.35 MPa. Both the weight of the porcine and bovine tissues reduced to 50% when the pressure reached 2.1 MPa.

By comparing the results for porcine and bovine tissue, we can specify two critical pressures (P1 and P2) that illustrate the change in RI under pressure. With the condition of no pressure, the tissue fluid on the surface of the sample has a higher RI because of evaporation and dehydration. When the applied pressure reached the first critical pressure P1 (in our experiment, ~0.35 MPa), the tissue fluid on the surface of the prism flowed away parallel to the surface of the sample, so a clear decrease of the proportion of tissue fluid was observed. The inner fluid of the sample flowed out and diluted the surface fluid, and the RI of

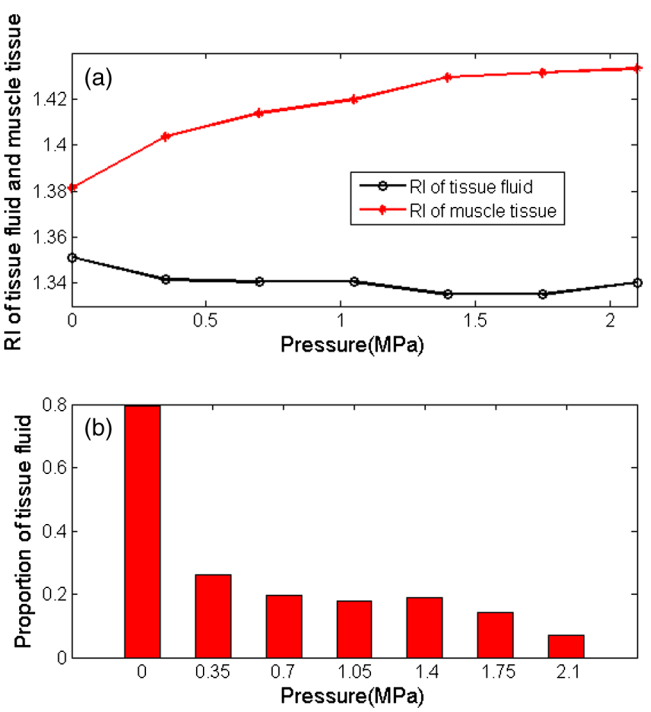

Fig. 3 (a) RIs of tissue fluid and bovine tissue versus the applied pressure. (b) Proportions of tissue fluid under different pressure.

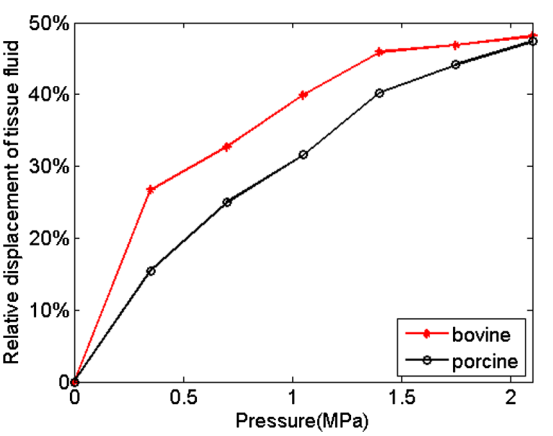

Fig. 4 Relative displacement of tissue fluid with different pressure.

tissue fluid decreased, too. The RI of tissue continually increased with the applied pressure. When the applied pressure reached the second critical pressure P2 (in our experiment, ~1.4 MPa), an increase in the proportion of tissue fluid was observed, which may be attributed to the rupture of cell membranes and the exudation of intracellular fluid. After this increase, both n_f and n_m increased, while the amount of tissue fluid reduced to a minimal level. A slight change in n_f and a continuous increase in n_m were observed during the complete compression process. The initial proportion of tissue fluid had a close relationship to sample preparation. The condensation of water on the sample surface during the sample defrosting process was inevitable, and hence, the proportion of tissue fluid at 0 MPa was not a good indication of the intrinsic sample condition. From 0.35 to 2.1 MPa, the speed of the reduction in tissue fluid at a constant pressure for bovine tissue is considerably faster than that for porcine tissue. This observation implies that water loss for bovine tissue under pressure occurs much more readily.

The disparity in the RI values under different compressions indicates that the tissue sample preparation, condition of the prism-sample interface, and intrinsic character of the tissue sample (water content, texture, hardness, and so on) have a significant impact on the final result. The deformation of the cell, displacement of water from collagen fibril, the increase of protein, sugar, and local chromophore concentrations, all contribute to the increase in the RI of muscle tissue under compression.[10–12]

This result also provides an evidence for the RI-matching mechanism of mechanical OC technique from another viewpoint. Since scattering arises from a mismatch in RI, organelles and subcomponents of organelles that have a different RI from their surroundings are expected to be the primary sources of cellular scattering.[20] Under certain amounts of compression, an obvious reduction in tissue fluid at the prism-tissue interface yields a higher RI in the contact area, which leads to mechanical OC. This study has also verified that dehydration is an important candidate mechanism for OC and can lead to the matching of the RI for intrinsic structures.[7]

4 Conclusion

In conclusion, the amount of pressure applied to the tissue sample affects the RI of muscle tissue and the amount of tissue fluid. An analytical model based on DTRM enables the simultaneous extraction of the change in RI and the proportion of tissue fluid at the contact area. The RI value can be regarded as one important parameter for selecting the proper experimental condition and for evaluating the effect of mechanical OC. In this work, we also report the quantitative values of the RI of compressed biotissue. Considering the recent interest in studies on tissue dynamics under mechanical stimuli, we expect to be able to expand this work by studying more tissue samples with respect to tissue dynamics, optical diagnosis, and treatment.

Acknowledgments

This research is supported by the Chinese National Key Basic Research Special Fund (Grant No. 2011CB922003), Science and Technology Program of Tianjin (Grant No. 11ZCKFSY00500).

References

1. V. V. Tuchin et al., "Light propagation in tissues with controlled optical properties," *J. Biomed. Opt.* **2**(4),401–417 (1997).
2. E. A. Genina, A. N. Bashkatov, and V. V. Tuchin, "Tissue optical immersion clearing," *Expert Rev. Med. Devices.* **7**(6), 825–842 (2010).
3. G. Vargas et al., "Use of an agent to reduce scattering in skin," *Lasers Surg. Med.* **24**(2), 133–141 (1999).
4. R. K. Wang et al., "Concurrent enhancement of imaging depth and contrast for optical coherence tomography by hyperosmotic agents," *J. Opt. Soc. Am. B* **18**(7), 948–953 (2001).
5. H. Kang et al., "Evaluation of laser beam profile in soft tissue due to compression, glycerol, and micro-needling," *Lasers Surg. Med.* **40**(8), 570–575 (2008).
6. A. Izquierdo-Román et al., "Erratum: mechanical tissue optical clearing technique increases imaging resolution and contrast through ex vivo porcine skin," *Lasers Surg. Med.* **43**(10), 814–823 (2011).
7. C. Drew, T. E. Milner, and C. G. Rylander, "Mechanical tissue optical clearing devices: evaluation of enhanced light penetration in skin using optical coherence tomography," *J. Biomed. Opt.* **14**(6), 064019 (2009).
8. W. C. Vogt et al., "Effects of mechanical indentation on diffuse reflectance spectra, light transmission, and intrinsic optical properties in ex vivo porcine skin," *Lasers Surg. Med.* **44**(4), 303–309 (2012).
9. J. Chaiken et al., "Instrument for near infrared emission spectroscopic probing of human fingertips in vivo," *Rev. Sci. Instrum.* **81**(3), 034301 (2010).
10. H. Shangguan et al., "Pressure effects on soft tissues monitored by changes in tissue optical properties," *Proc. SPIE* **3254**, 366–371 (1998).
11. E. K. Chan et al., "Effects of compression on soft tissue optical properties," *IEEE J. Sel. Top. Quantum Electon.* **2**(4), 943–950 (1996).
12. R. Reif et al., "Analysis of changes in reflectance measurements on biological tissues subjected to different probe pressures," *J. Biomed. Opt.* **13**(1), 010502 (2008).
13. Z. Wang et al., "Tissue refractive index as marker of disease," *J. Biomed. Opt.* **16**(11), 116017 (2011).
14. B. Wang et al., "Dynamic schema for near infrared detection of pressure-induced changes in solid tumors," *Appl. Opt.* **47**(16), 3053–3063 (2008).
15. H. F. Ding et al., "Refractive indices of human skin tissues at eight wavelengths and estimated dispersion relations between 300 and 1600 nm," *Phys. Med. Biol.* **51**(6), 1479–1489 (2006).
16. J. Wang et al., "Effect of tissue fluid on accurate determination of the complex refractive index of animal tissue," *J. Biomed. Opt.* **17**(7), 075011 (2012).
17. M. Born and E. Wolf, *Principles of Optics*, Pergamon, New York (1959).
18. H. Li and S. S. Xie, "Measurement method of the refractive index of biotissue by total internal reflection," *Appl. Opt.* **35**(10), 1793–1795 (1996).
19. J. J. J. Dirckx, L. C. Kuypers, and W. F. Decraemer, "Refractive index of tissue measured with confocal microscopy," *J. Biomed. Opt.* **10**(4), 044014 (2005).
20. R. Drezek, A. Dunn, and R. Richards-Kortum, "Light scattering from cells: finite-difference time-domain simulations and goniometric measurements," *Appl. Opt.* **38**(16), 3651–3661 (1999).